Influence of impeller vane arrangement on efficiency performance and pressure fluctuations of a double-suction centrifugal pump

Influence of impeller vane arrangement on efficiency performance and pressure fluctuations of a double-suction centrifugal pump

SONG Yu [1,*], LUO Yongyao [2]

1. Institute of Nuclear and New Efficiency Technology, Tsinghua University, Beijing 100084, China.

Collaborative Innovation Center of Advanced Nuclear Efficiency Technology, Key Laboratory of Advanced Reactor Engineering and Safety, Ministry of Education of China.

2. State Key Laboratory of Hydroscience and Engineering, Department of Energy and Power Engineering, Tsinghua University, Beijing 100084, China.

* Corresponding author E-Mail: labfmfe@163.com; Tel.: +86-10-6278-0605.

Abstract. Two double-entry impellers with inline-vane and staggered-vane arrangements are designed, and then the influence of impeller-vane arrangement on efficiency performance and pressure fluctuations of a double-suction centrifugal pump is investigated. The reliability and accuracy of the numerical method is validated by comparing the experimental and numerical results of pump efficiency performance. The relative error of efficiency at four different flow rates is below 3%. The efficiency performance for different vane arrangements are compared. Eighteen monitoring locations covering important pump regions in impeller and volute are set to obtain the details of pressure fluctuations. The results show that the pressure fluctuations in the volute is greatly reduced for staggered-vane arrangement. The pressure distributions at middle-span plane of the pump show smaller pressure variation for staggered-vane impeller. The overall investigation reveals a weaker rotor-stator interaction for the staggered-vane impeller.

1. Introduction

Flow in centrifugal pumps involve turbulence, secondary flows, unsteadiness. Moreover, the geometry of the volute is complex and asymmetric, which generates an unsteady interaction with the impeller. As a result, the operation of centrifugal pumps can result in the generation of instabilities and pressure pulsations, which can affect the mechanical integrity of the pump, resulting in excessive vibration and/or noise. In recent years, considerable work has been done to study the unsteady interaction in centrifugal pumps, numerically and experimentally. Parrondo et al. [1] conducted a systematic series of experiments to measure the pressure fluctuations on 36 points around the volute of a centrifugal pump for flow rates from 0% to 160% of the design flow condition. The experimental data indicate that the pressure fluctuations result from the superposition of the hydraulic disturbances and the rotor-

stator interaction. Pavesi et al. [2] led an experimental investigation of the flow instability in a centrifugal pump. The results revealed the existence of an asymmetrical rotating pressure structure at the impeller outlet, which was related to the phenomenon of jet-wake. Majidi [3] solved the unsteady three-dimensional viscous flows in a centrifugal pump to obtain the unsteady pressure distribution in the impeller and volute. The results show that the pressure fluctuations are strong at impeller outlet and at the vicinity of the volute tongue, due to the interaction between impeller and volute. Li [4] investigated the effect of blade exit angles and liquids on pressure and velocity pulsations in centrifugal pump by means of experiment and numerical simulation. The results reveal that a larger fluid viscosity and a smaller blade exit angle can reduce the fluctuation of flow variables.

Double-suction pumps are used in applications where high flow is required in a single stage pump. In double-suction pumps, the two set of vanes are arranged back-to-back, which minimizes the net axial forces on the shaft. However, due to the high energies involved, double-suction and double volute, these pumps usually suffer more complex from pressure pulsations than single entry pumps. Spence et al. [5, 6] provided a wider parametric study to investigate the effect of various geometries features on the pressure pulsations in a double-suction pump. The investigation had taken the form of a parametric study covering four geometric parameters: the cutwater gap, vane arrangement, snubber gap and the sidewall clearance. The pressure pulsations were investigated on three different flow rates at 15 different locations covering important pump regions. The cutwater gap and vane arrangement is found to be the greatest influence on the pressure pulsations. Pressure pulsations at the top dead centre of the pump volute casing reveal a better indication of internal pump pulsations than that at the discharge. Al-Qutub et al.[7] explored the effect of V-Shaped cut at blade exit of a double volute centrifugal pump. The results show that the V-cut increases the effective gap between the trailing edge of the impeller blades and volute tongue and reduces the rotor-stator interaction, which is the cause of pressure pulsation in the pump. However, the V-cut brings an adverse effect on pump performance (5% reduction in head) at rated flow rate.

Studies on the complex flow and pressure pulsation are of great significance for improving stability of a double-suction pump. Therefore, in the present research, the pressure pulsations and flow behaviors in two different impeller vane arrangements are investigated and compared by performing simulations involving the complete hydraulic pump geometry.

2. Physical Model And Numerical Method

2.1. Physical model of centrifugal pump

The tested double-suction pump is a commercial single stage centrifugal pump with six backward blades. Figure 1 shows the tested centrifugal pump. Figure 2 shows the three-dimensional model of entire computational flow passage. The main design parameters of the double-suction pump are listed in Table 1.

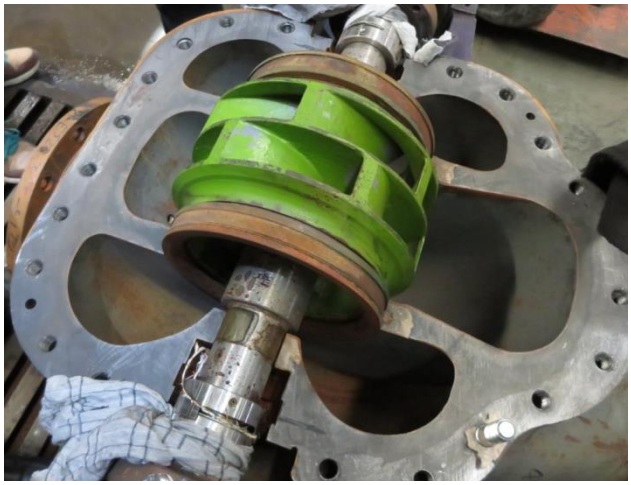

Figure 1. Tested double-suction centrifugal pump.

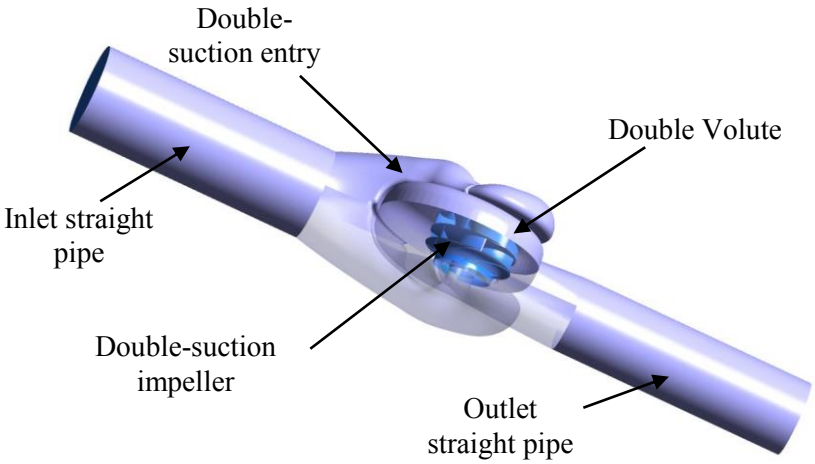

Figure 2. The computational domain of the centrifugal pump.

Table 1. Key parameters for the mixed-flow pump.

Parameter	Value
Rated Flow Rate Q (m^3/h)	864
Rated Head H (m)	17.8
Rotational Speed n (r/min)	1480
Specific Speed n_s (-)	215.9
Number of impeller blade Z_i (-)	6
Diameter of impeller inlet D_1 (mm)	198
Diameter of impeller outlet D_2 (mm)	286
Diameter of inlet straight pipe (mm)	300
Diameter of outlet straight pipe (mm)	250

2.2. Computational mesh of centrifugal pump

The computational domain is composed of five parts: the inlet straight pipe, double-suction entry, double-suction impeller, double volute and outlet straight pipe, as shown in Figure 2. Two different impeller vane arrangements are considered, an inline-vane arrangement, a mid position staggered-vane (30°) arrangement. The meshes of two different impellers, volute and suction are shown in Figure 3. The impeller structure mesh is generated using CFX-Turbogrid. The volute and suction unstructured meshes are generated using ICEM, which are refined near the tongue region individually.

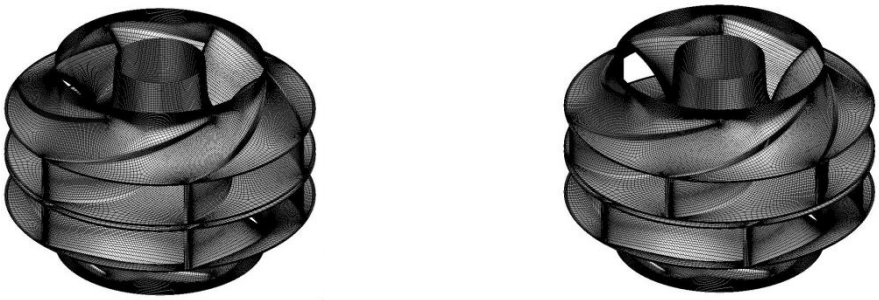

(a) Inline-vane impeller mesh (b) Staggered-vane impeller mesh

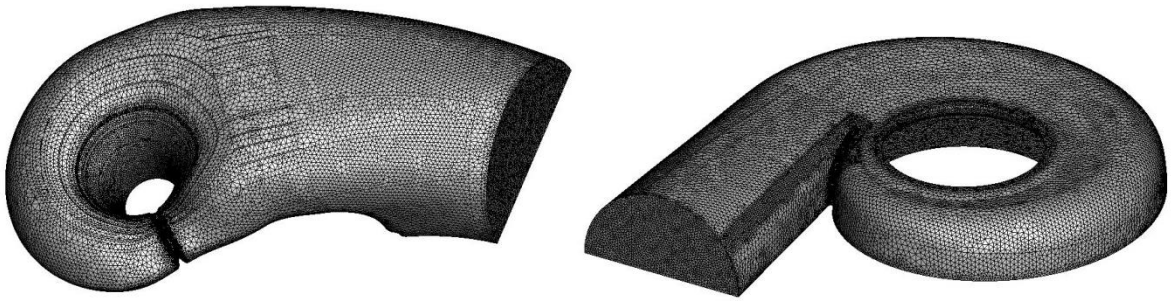

(c) Suction mesh (d) Volute mesh

Figure 3. Mesh of different part in pump.

3. Numerical Method And Validation

The computation fluid dynamics software CFX 14.5 is conducted to simulate the flow in the pump. Turbulence is modeled with a RNG *k*-*ε* model [8]. The present work is conducted using total pressure at inlet and a mass flow at outlet as the set of boundary conditions [9]. The no-slip boundary conditions [10] are imposed at the inlet straight pipe, suction wall, the blade pressure and suction surfaces, the impeller hub and shroud, the volute wall and outlet straight pipe. The interfaces between rotating and stationary frames are modelled using the frozen-rotor and transient-rotor stator interface option for steady and unsteady calculations, respectively [11, 12]. The steady-state is simulated as the initial flow field of the unsteady simulation. Y+ values are greater than 60 in the important flow region and the logarithmic law-of-the-wall is used to predict near the wall characteristics. The convergence criterion is defined as that the root-mean-square residual for each equation at the end of each time step is below 1×10^{-5}[13-16]. All calculations were conducted in a server with two CPUs of Intel ES-2643 3.4 GHz processor, 64 GB RAM, and 2 TB hard drive.

Five sets of meshes with elements from 3,436,239 to 5,405,583 are employed to validate the grid independence, as shown in Table 2. The test results reveal that the variation of pump head $\Delta H/H1$ and efficiency $\Delta\eta/\eta_1$ is slight (less than 0.002), as shown in Figure 4. Considering computational cost and accuracy, Mesh 3 with 4,398,195 elements is adopted in the following research. The run time for steady state is about 86400s.

Table 2. Mesh sizes for mesh independency test.

Item	Mesh 1	Mesh 2	Mesh 3	Mesh 4	Mesh 5
Inlet pipe	141777	141777	141777	141777	141777
Outlet pipe	90068	90068	90068	90068	90068
Impeller	531036	1013796	1492992	2018520	2500380
volute	1511542	1511542	1511542	1511542	1511542
suction	1161816	1161816	1161816	1161816	1161816
Whole passage	3436239	3918999	4398195	4923723	5405583

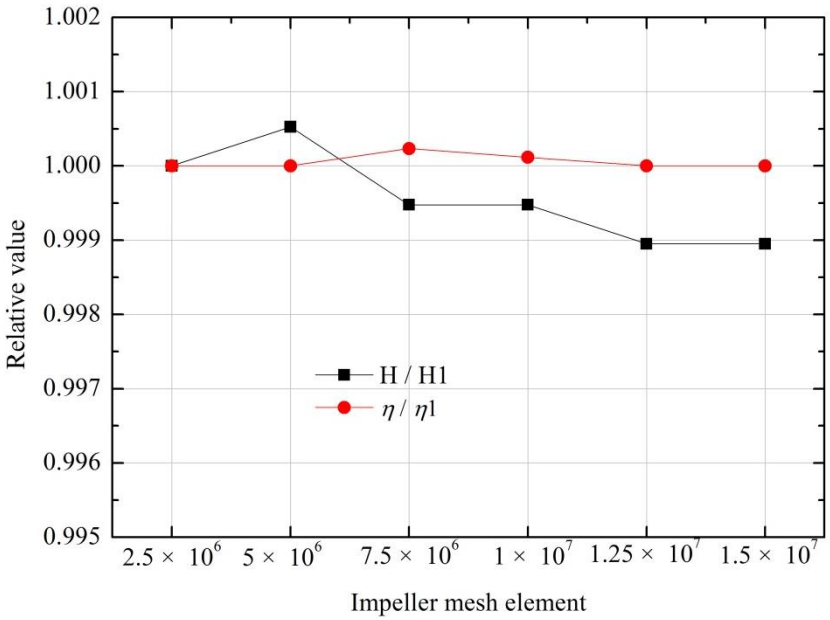

Figure 4. Mesh independency test.

The time step for transient runs is 2.1115×10^{-4} *s*, as this provided 192 time steps per impeller rotation (32 time steps per blade passage). This time step is chosen based upon the numerous previous work related to pumps [13-16].

The experiment of tested pump is conducted on the test apparatus in East Pump Co., Ltd, Shanghai, China. A comparison of the CFD results with the experiments in head and efficiency is given in Figure 5 at four different flow rates. The relative error of efficiency at the four flow rate is concluded in Table 3. The relative error of efficiency at design flow rate is below 2%, while at partial and over loads, the errors are still below 3%.

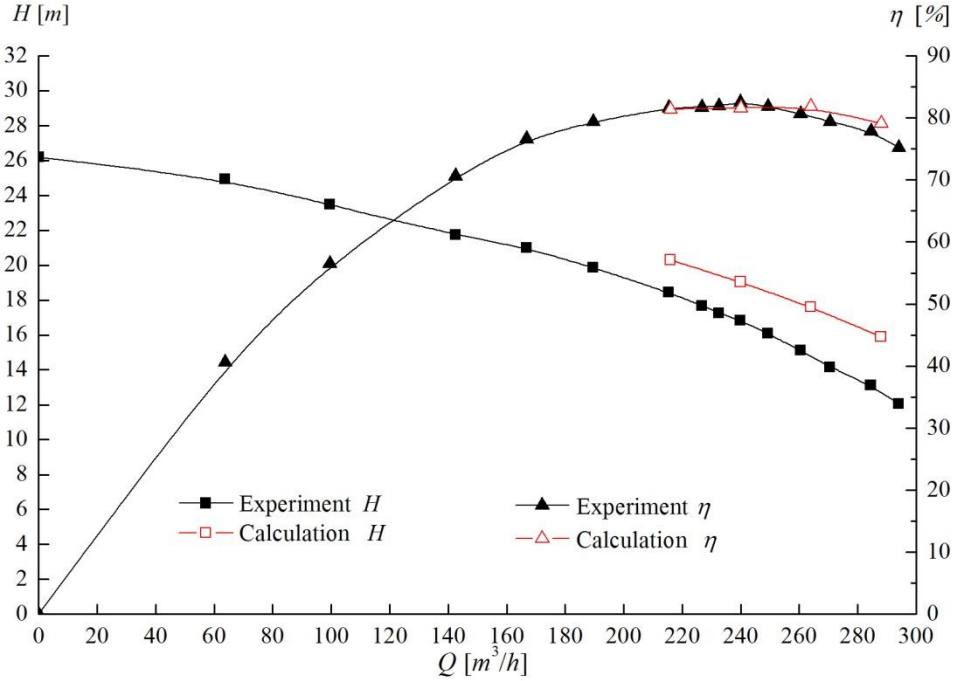

Figure 5. Comparison of pump performance between experiment and calculation results.

Table 3. Relative error of the efficiency.

Q[m^3/h]	216	240	264	288
relative error[%]	0.27638	1.12537	2.03071	2.8844

4. Results and discussions

To investigate the unsteady flow in the impeller, and volute of the centrifugal pump, 18 monitoring points are set, including: IPS1-4 on blade pressure side, ISS1-4 on blade suction side corresponding to the same position of IPS1-4 and V1-10 on volute wall from tongue to outlet, as shown in Figure 6(a-c).

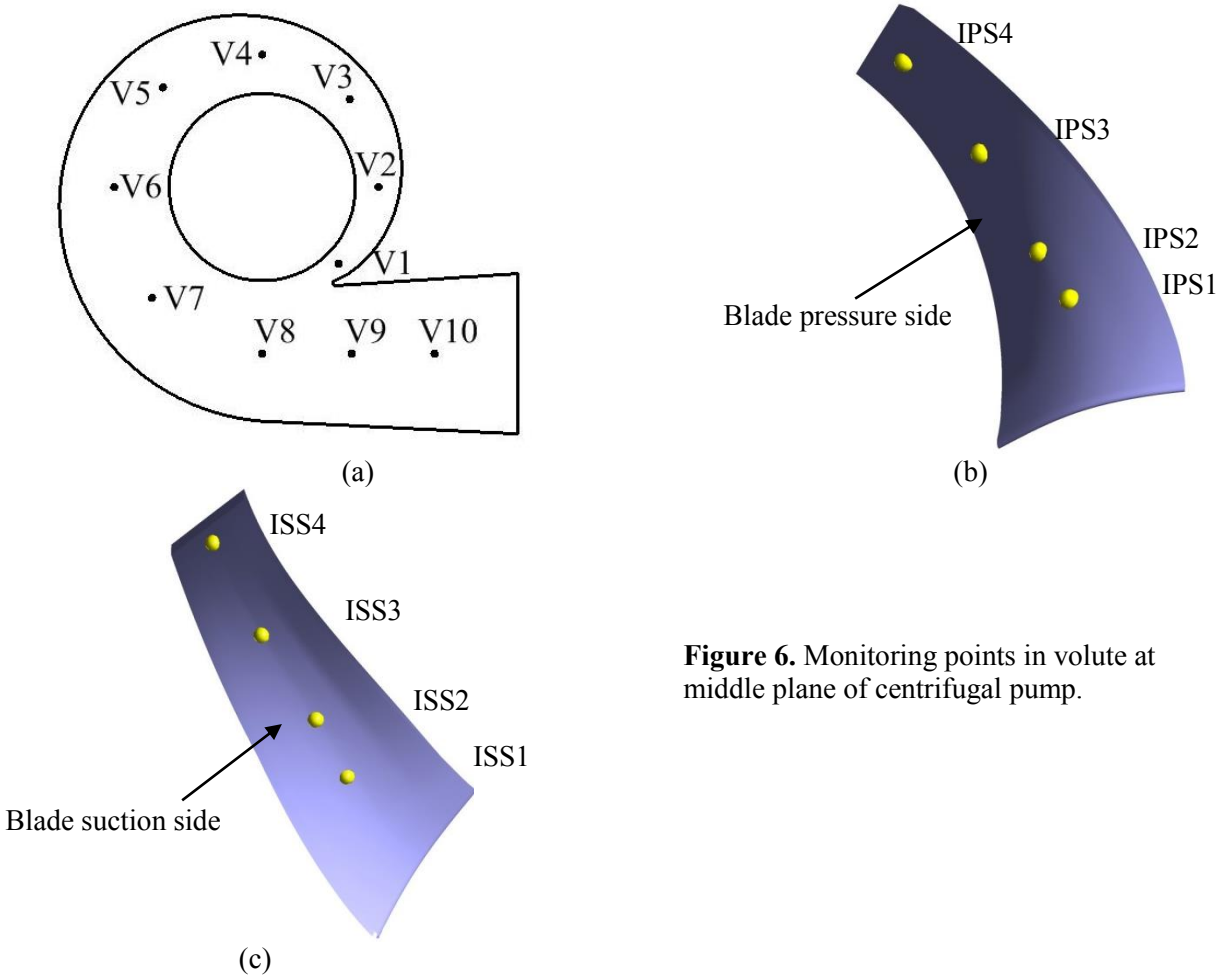

Figure 6. Monitoring points in volute at middle plane of centrifugal pump.

4.1. Q, H, η performance in centrifugal pump

Figure 7 shows the Q, H, η performance of the centrifugal pump for the two different vane arrangements at four different flow rates. As shown in the figure, the efficiency for staggered-vane arrangement is basically the same as the inline-vane arrangement. The maximum deviation is 1.06%. While the head for staggered-vane arrangement is a little higher, with the maximum deviation 1.13%.

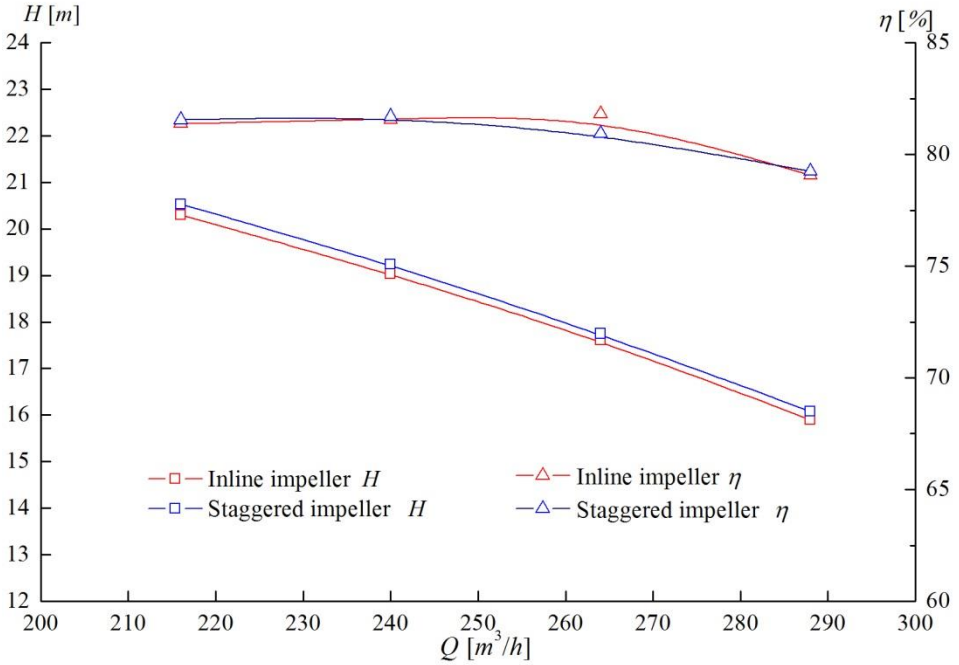

Figure 7. Q, H, η performance of centrifugal pump for the different arrangements.

4.2. Pressure fluctuations

The transient calculation is conducting more than 15 impeller revolutions. The pressure fluctuations on monitoring points are observed. The data of last 10 cycles is used to make the Fast Fourier transform (FFT) to obtain the frequency characteristics of pressure fluctuation on monitoring points.

Figure 8 shows the pressure fluctuations spectrums on monitoring points V1-10 on volute for the different impeller-vane arrangements. For inline-vane arrangement, there are clearly two harmonics. The dominant frequencies of pressure fluctuations on those monitoring points are the blade passing frequency $f_{BPF} = n \times z / 60 = 148$, the amplitudes of which are obviously larger than the other harmonics with frequency $2f_{\mathrm{BPF}}$. The pressure fluctuation amplitudes on monitoring points V1 and V2 are extraordinarily larger than that on other points. For staggered-vane arrangement, the dominant frequencies of pressure fluctuations on those monitoring points are $2f_{\mathrm{BPF}}$, which is second largest harmonics for inline-vane arrangement. The pressure fluctuation amplitudes on monitoring points V1-V10 at this frequency are almost the same as that for inline-vane arrangement. Compared with inline-vane arrangement, the pressure fluctuation at f_{BPF} is significantly reduced, which is the main cause of the vibration in volute.

Figure 9 shows the pressure fluctuations spectrums on monitoring points IPS1-4 and ISS1-4 on impeller for different vane arrangements. For both inline-vane and staggered-vane arrangement, the dominant frequencies of pressure fluctuations on IPS1-4 and ISS1-4 monitoring points are near the impeller rotation frequency $f_i = n / 60 = 24.67$. The harmonics distribution and amplitudes are almost the same.

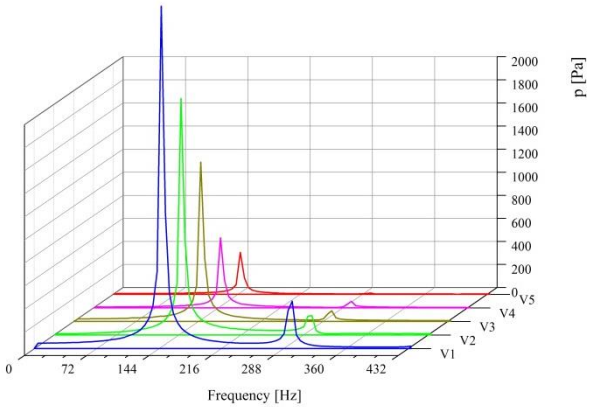

(a) V1-5, inline-vane impeller

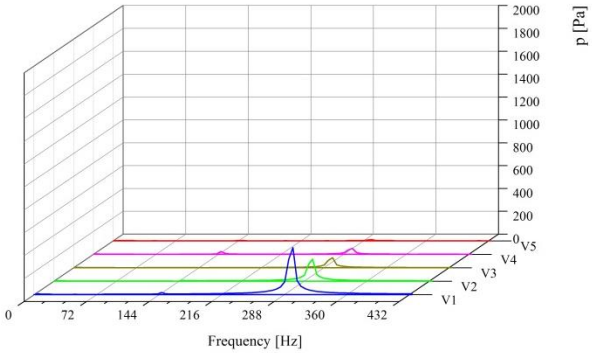

(b) V1-5, staggered-vane impeller

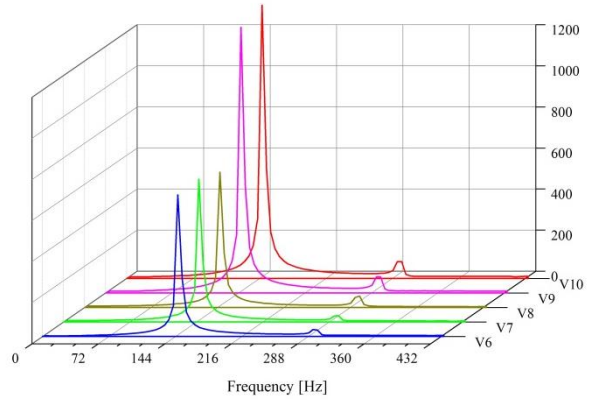

(c) V6-10, inline-vane impeller

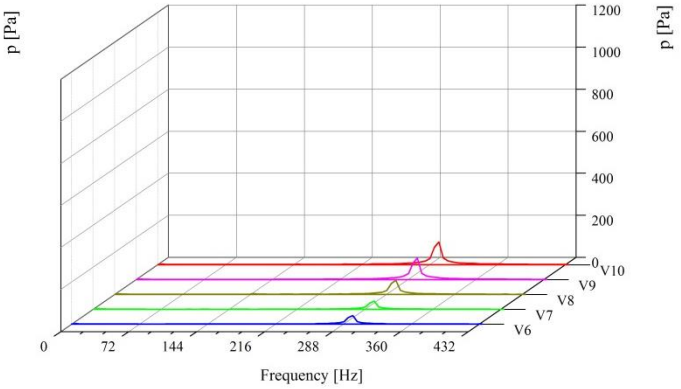

(d) V6-10, staggered-vane impeller

Figure 8. Spectrum analysis of pressure fluctuation on V1-10 for different impeller-vane arrangements.

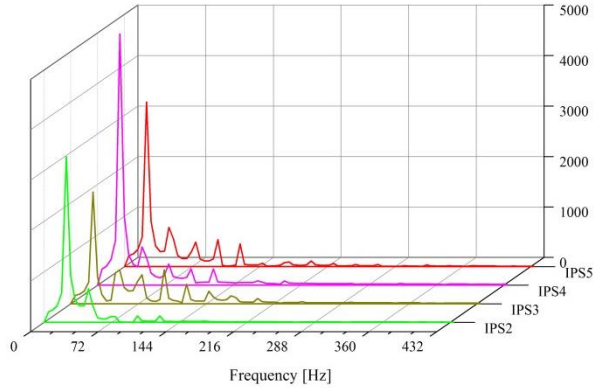

(a) IPS1-4, inline-vane impeller

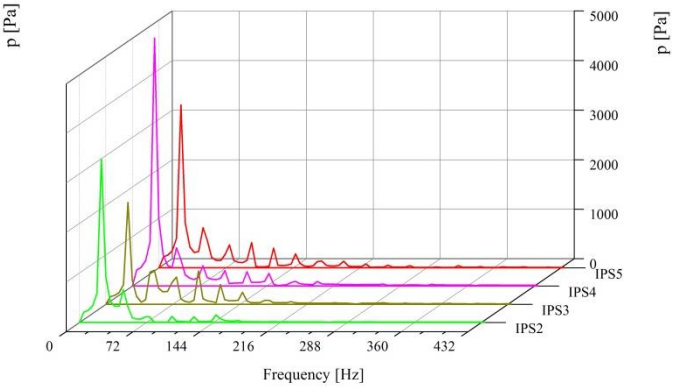

(b) IPS1-4, staggered-vane impeller

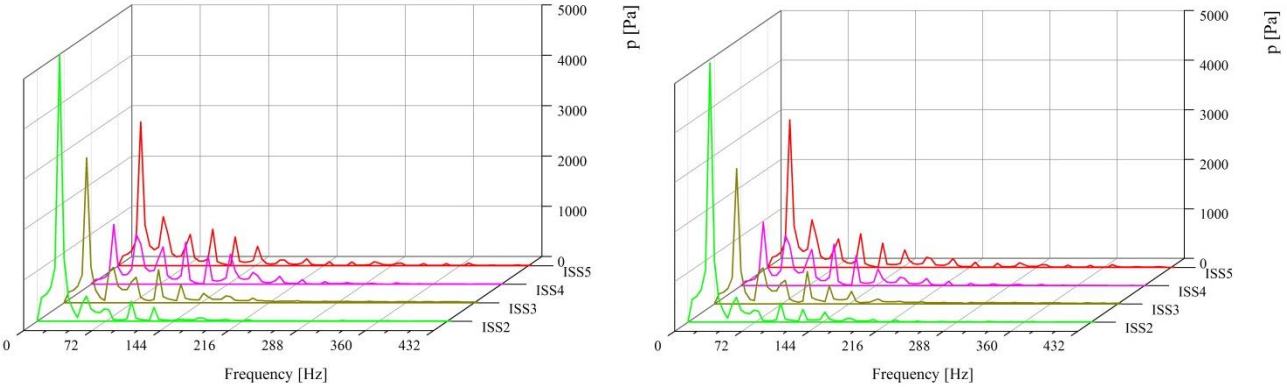

(c) ISS1-4, inline-vane impeller (d) ISS1-4, staggered-vane impeller

Figure 9. Spectrum analysis of pressure fluctuation on IPS1-4 and ISS1-4 for different impeller-vane arrangements.

Table 4 shows the dominant frequencies and maximum amplitudes of pressure fluctuations on V1-10, IPS1-4 and ISS1-4.

Table 4. Spectrum analysis of pressure fluctuations on V1-10, IPS1-4 and ISS1-4.

	Dominant Frequency/Hz		Maximum Amplitude /Pa	
Monitoring Point	Inline-vane	Staggered-vane	Inline-vane	Staggered-vane
V1	146.67	298.07	2966.63	112.85
V2	146.67	298.07	2049.19	53.66
V3	146.67	298.07	1382.73	24.10
V4	146.67	298.07	608.64	14.87
V5	146.67	298.07	363.69	3.12
V6	146.67	298.07	689.20	11.25
V7	146.67	298.07	695.51	10.88
V8	146.67	298.07	659.98	18.84
V9	146.67	298.07	1293.89	28.31
V10	146.67	298.07	1329.15	30.11
IPS1	23.66	23.66	3285.22	3303.06
IPS2	23.66	23.66	2212.07	2053.73
IPS3	23.66	23.66	4977.80	5002.67
IPS4	23.66	23.66	3265.87	3291.39
ISS1	23.66	23.66	5293.05	5232.11
ISS2	23.66	23.66	2884.82	2732.32
ISS3	23.66	23.66	1189.23	1278.21
ISS4	23.66	23.66	2858.18	2982.07

4.3. Pressure distribution in volute

The flow field in the monitor region of volute is studied for the different impeller-vane arrangements. Figure 10 shows the instantaneous pressure distribution at middle-span plane of the pump from t = 0.751692 to 0.783787 (s) corresponding to 1/6 impeller revolution time, that is, the time of a blade passing the volute tongue. The four sequent maps demonstrate the pressure details at middle-span plane due to the interaction between the impeller and the volute. The left side and right side of the graph are pressure distribution for inline-vane and staggered-vane impeller, respectively.

As shown in Figure 10, for inline-vane impeller, the region of high pressure near the volute tongue is greater at t = 0.75507 and 0.75676 (s) than that for the staggered-vane impeller. The blade effect near the volute inlet is relatively evident, resulting from the interaction between the impeller and the volute. The pressure variations are obviously shown at different time, especially near the volute outlet.

For staggered-vane impeller, the pressure distribution at middle-span plane is nearly the same, which reveals a weaker rotor-stator interaction.

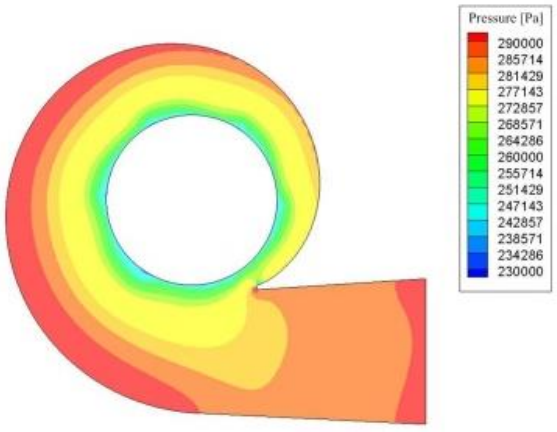

(a) t =0.751692 s, inline-vane impeller

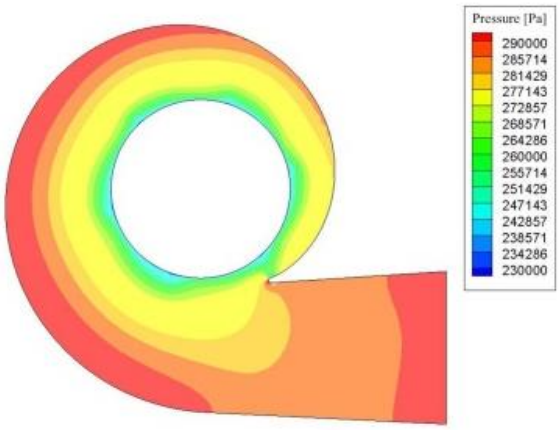

(b) t =0.753381 s, inline-vane impeller

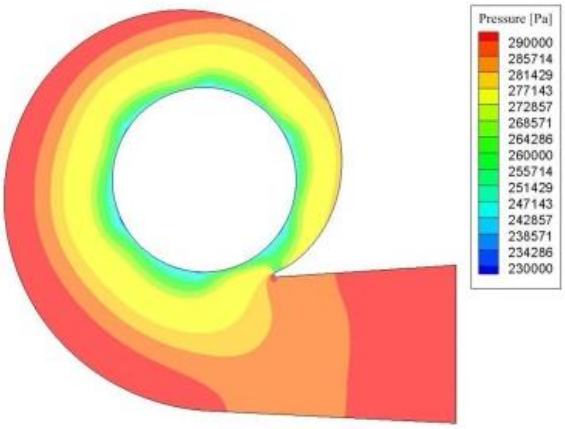

(c) t =0.75507 s, inline-vane impeller

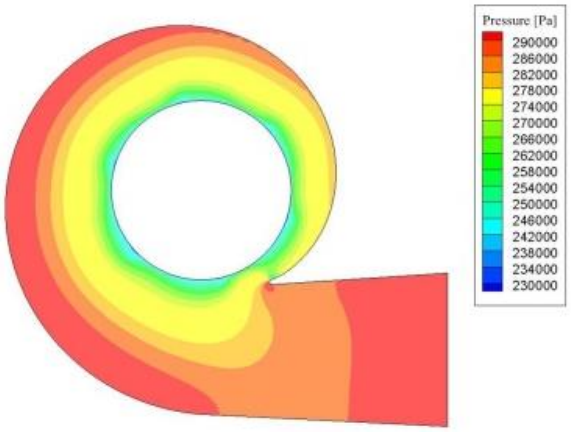

(d) t =0.75676 s, inline-vane impeller

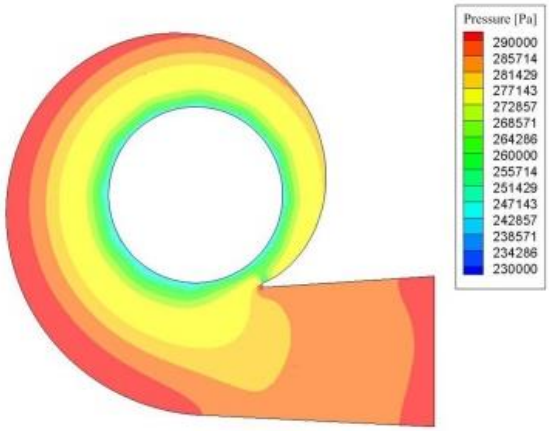

(e) t =0.751692 s, staggered-vane impeller

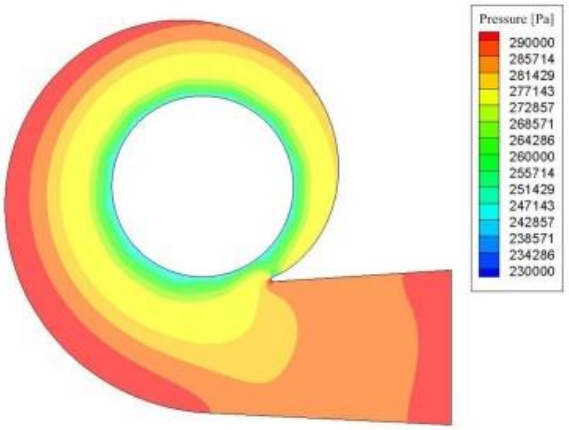

(f) t =0.753381 s, staggered-vane impeller

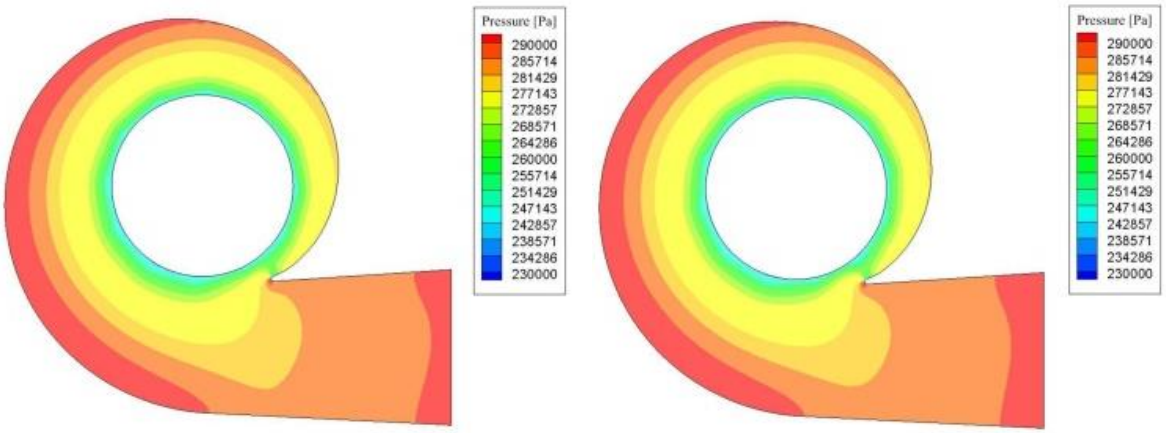

(g) t =0.75507 s, staggered-vane impeller (h) t =0.75676 s, staggered-vane impeller

Figure 10. Instantaneous pressure distribution at middle-span plane.

5. Conclusion

In the present paper, the impact of impeller-vane arrangements on Q, H, η performance, pressure fluctuations and pressure distribution of a double-suction centrifugal pump is studied. Based on the numerical simulations and analysis results, we conclude as follows:

(1) The influence of impeller-vane arrangement on efficiency performance is slight.

(2) The dominant frequencies of pressure fluctuations on the monitor points in volute are different for different impeller-vane arrangements, f_{BPF} for inline-vane impeller and 2 f_{BPF} for staggered-vane impeller. Compared with the inline-vane arrangement, the pressure fluctuations at f_{BPF} is reduced for staggered-vane arrangement and the maximum value of pressure fluctuations is much weaker.

(3) For inline-vane impeller, the region of high pressure near the volute tongue at middle-span plane is greater at t = 0.75507 and 0.75676 (s) than that for the staggered-vane impeller. The blade effect near the volute inlet is relatively evident. The pressure variations at different time are obvious, especially near the volute outlet. While, the pressure distribution for staggered-vane impeller is nearly the same.

(4) The staggered-vane arrangement influences the pressure fluctuations and pressure distribution in the volute and results in a weaker rotor-stator interaction.

6. Acknowledgments

This work has been supported by the Tsinghua University Initiative Scientific Research Program [Grant number 20151080376], the National Natural Science Foundation of China [51741906], the Open Research Fund Program of State key Laboratory of Hydroscience and Engineering [sklhse-2018-E-01], the State Key Laboratory of Hydroscience and Engineering [2018-KY-02], and the Key Laboratory of Fluid and Power Machinery (Xihua University), Ministry of Education [szjj-2017-100-1-004].

References

[1] Parrondo-Gayo J L, Gonzalez-Perez J and Fernandez-Francos J 2002 *J. Fluids Eng.* **124** 784–90.
[2] Pavesi G, Cavazzini G and Ardizzon G 2008 *Int. J. Heat. Fluid. Fl.* **29** 1527–40.
[3] Majidi K 2005 *J Turbomach* **127** 363–71.
[4] Li W G 2012 *Proc. Inst. Mech. Eng. Part A J. Power Efficiency* **226** 580–99.
[5] Spence R, Amaral-Teixeira J 2009 *Computers and Fluids* **38** 1243–57.
[6] Spence R, Amaral-Teixeira J 2008 *Computers and Fluids* **37** 690–704.
[7] Al-Qutub, Amro M, Khalifa, Atia E, Al-Sulaiman and Faleh 2012 *A Journal of Pressure Vessel*

Technology, Transactions of the ASME **134** 021301.
[8] Argyropoulos C D and Markatos N C 2014 *Applied Mathematical Modelling* **39** 693–732.
[9] Tan L, Zhu B and Cao S 2014 *Proceedings of the Institution of Mechanical Engineers, Part C: Journal of Mechanical Engineering Science* **228** 1994–2006.
[10] Liu Y, Tan L, Liu M, Hao Y and Xu Y 2017 *Energies* **10** 695.
[11] Hao Y, Tan L, Liu Y, Xu Y, Zhang J and Zhu B 2017 *Energies* **10** 57.
[12] Liu Y, Tan L, Hao Y and Xu Y 2017 *Energies* **10** 191
[13] Tan L, Zhu B and Wang Y 2015 *Engineering Computations* **32** 1549–66.
[14] Wang Y, Tan L and Zhu B 2015 *Proceedings of the Institution of Mechanical Engineers, Part C: Journal of Mechanical Engineering Science* **18** 3405–16.
[15] Tan L, Yu Z, Xu Y, Liu Y and Cao S 2017 *Proceedings of the Institution of Mechanical Engineers Part A Journal of Power & Energy* **231** 227–38.